



# Wood Plastic Composites from the Waste Lignocellulosic Biomass Fibers of Bio-Fuels Processes: A Comparative Study on Mechanical Properties and Weathering Effects

Bo Chen<sup>1</sup> · Zhangfeng Luo<sup>1</sup> · Huidong Chen<sup>2,3</sup> · Changjing Chen<sup>1</sup> · Di Cai<sup>1</sup> · Peiyong Qin<sup>1</sup> · Hui Cao<sup>1</sup> · Tianwei Tan<sup>1</sup>

Received: 7 April 2018 / Accepted: 23 July 2018 / Published online: 26 July 2018  
© Springer Nature B.V. 2018

## Abstract

Using the lignocellulosic biomass materials to produce wood (wood fibers/natural fibers) plastic composites (WPCs) is one of the most environmentally friendly and economical ways to solve the residuals of biorefineries. In this study, tropical maize bagasse (TMB), sweet sorghum bagasse (SSB) and sugarcane bagasse (SCB), the solid residuals from bio-ethanol plants, were used as the reinforcement phase in the production of WPCs. The mechanical, thermal and accelerated weathering behaviors of WPCs were evaluated. The experimental results indicated that the TMB reinforced composites showed better mechanical properties, with tensile strength and flexural strength of  $26.8 \pm 3.4$  and  $46.1 \pm 3.1$  MPa, respectively. Moreover, the retention ratios of the rupture modulus and the elasticity modulus of the SSB reinforced composites were the highest among the three groups after multigelation and 2000 h of xenon lamp weathering, which were reached  $84.9 \pm 6.7$  and  $76.0 \pm 4.4\%$ , and  $76.1 \pm 4.7$  and  $69.4 \pm 2.9\%$ , respectively. The production of WPCs reinforced by solid residuals showed potential in connecting with the biorefinery plants.

**Keywords** Lignocellulosic biomass fiber · Wood plastic composite · Mechanical property · Weathering effect

## Statement of Novelty

The current work provides a novel process for woody plastic composite production using the solid residual after bioethanol production. The effect of different types of fibers include

tropical maize bagasse, sweet sorghum bagasse and sugarcane bagasse that obtained after squeezing and utilizing the fermentable juices on physical mechanisms of WPCs were compared. The weathering effect of the three kinds of fibers reinforced WPCs were also compared for the first time.

**Electronic supplementary material** The online version of this article (<https://doi.org/10.1007/s12649-018-0413-8>) contains supplementary material, which is available to authorized users.

✉ Di Cai  
caidibuct@163.com

✉ Hui Cao  
caohui@mail.buct.edu.cn

<sup>1</sup> National Energy R&D Center for Biorefinery, Beijing University of Chemical Technology, No.15 Beisanhuan East Road, Chaoyang District, Beijing 100029, People's Republic of China

<sup>2</sup> College of Chemical Engineering, Beijing University of Chemical Technology, Beijing 100029, People's Republic of China

<sup>3</sup> Center for Process Simulation & Optimization, Beijing University of Chemical Technology, Beijing 100029, People's Republic of China

## Introduction

Wood (wood fibers/natural fibers) plastic composites (WPCs), with advantages of low density, good mechanical and thermal insulation properties and availability, are considered as a type of sustainable low-cost material. With the development of economy, the demand for timber has been increasing, which makes the cutting of forest resources without planning, lead to the emergence of deforestation [1, 2]. Therefore, people seek for proper materials to replace woody products. In recent years, because of the shortage and the degradation of forest, there is an attempt using the fast growing lignocellulosic materials as alternative reinforcement candidates in WPCs manufacturing [3, 4]. In comparison with the woody biomass materials, WPCs reinforced by the agriculture residuals are considered as one of the most

attractive ways because of the low cost and ready availability [2]. More importantly, most of the agro-plants belong to gramineae, so the accumulation of biomass was always faster than numerous softwoods and hardwoods.

However, the direct application of agro-residuals as the reinforcing phase of WPC was limited by the costly raw materials supply chains [5]. In addition, it meets the economic competitions to the biorefinery processes for chemical and fuels production [6]. To address this problem, a potential method is extending the value chain of the conventional biorefinery process. That is, using the lignocellulosic biomass residuals of the bioprocesses, the by-products, as the reinforcement for the composites productions [7]. In literatures, the distillers dried grains with soluble (DDGS) after ethanol fermentation, the microalgae biomass, and the potato peel residue after fermentation have been used for the production of the composites [7–10]. In our previous study, the fermentation residual after sequential cellulosic ethanol and acetone–butanol–ethanol fermentations that contain lignin, protein and unhydrolyzed carbohydrates were also used as the reinforcing phase for WPCs [11].

Moreover, for the chemical production using lignocellulosic agro-residuals as raw materials, it was difficult to be industrialization because of the resistant of the lignocellulosic structure, environmental unfriendly pretreatment, cost-effective cellulase supplement, and the low tolerance to the inhibitors and products of strains [12–15]. By contrast, luckily, the sugar containing juice in fresh stalks, such as sugarcane, tropical maize and sweet sorghum, were proved as the low-cost and more feasible substrate for fermentative biochemical productions with high productivity and yields [11, 16, 17]. In that route, the cellulosic bagasse remaining was always burned to provide heat and electricity after utilizing the sugar containing juice for fermentative biofuels production. However, this route is not profitable [18, 19].

As a feasible route for maximizing the economic value of the lignocellulosic materials after utilizing the fermentable juices, previous studies were explored in detail for the production of WPCs using the solid residual after bioprocessing [11, 20]. However, to our knowledge, there are no researches focusing on comparison of the mechanical properties and weathering effects using different types of the lignocellulosic bagasse that remained after fermentation. Nevertheless, as it demonstrated previously, the differences of the fibers type, the chemical composition of the bagasse, the crystallinity of the cellulose hugely affect the mechanical and physical properties of WPC [2, 21, 22].

Here in, a comparison of the reinforced performances of sugarcane, tropical maize and sweet sorghum bagasses on WPCs production was evaluated in detail. The mechanical and physical properties of the WPCs reinforced by different types of fibers were evaluated, followed by the weathering tests. The results indicated that the bagasses of sugar crops,

the intractable solid residuals, in biorefinery processes could be used for the valuable biocomposites production rather than the low-valuable burning for heat, which showed promising in future industrial applications. In addition, this process successful extends the life cycle of biomass resources and improves the profitability of biorefinery.

## Materials and Methods

### Sugar Crops Bagasse and the Polyethylene

The fresh tropical maize stalk (Zhongnongdatian 419) was kindly provided by China Agricultural University and was harvested on an experimental field in Sep. 2016, City Zhuozhou, Hebei province of China. The sweet sorghum stalk (Chuntian 2) was kindly provided by Prof. Guiying Li from Chinese Academy of Agricultural Sciences and was harvested on an experimental field in Oct. 2016, Shunyi district, Beijing, China. The sugarcane (Guiguozhe 1) was purchased from local market in Beijing. The fermentable juices in the stalks were squeezed by a 3-rollermill (SY-20, Guangzhou Fukang Co. Ltd, China) within 24 h [17]. Juices were used for biofuels fermentation [11, 15], while the bagasse remained were collected and washed by deionized water, followed by dried out at 105 °C. The dried bagasses were then well milled into 40–60 meshes, and were stored in – 20 °C to protect them from invade and infect of microorganisms. The high density polyethylene (HDPE) was provided by Beijing Jinma Plastic Co. Ltd., China.

### Fibers Structure and Properties

The structure and properties of the tropical maize bagasse (TMB), sweet sorghum bagasse (SSB) and sugarcane bagasse (SCB) were analyzed by determine the chemical compositions, the morphology of fibers, the particle size distribution of fibers, the functional groups of fibers and the crystallinity of the cellulose.

For the determination of the fibers chemical compositions, the standard of NREL was applied [23]. Briefly, the bagasse was mixed well with 72% v/v H<sub>2</sub>SO<sub>4</sub> and rotated at room temperature for an hour, followed by dilution the H<sub>2</sub>SO<sub>4</sub> solution to 4% v/v and kept at 121 °C for an hour. The glucose derived from glucan and xylose derived from xylan were detected. Lignin can be analyzed by weighting the solid remain and the UV absorbancy of the liquid fraction obtained.

The SEM (SU1510, HITACHI, Japan) and particle size analyzer (Mastersizer 2000, Malvern, UK) was employed to test the morphology and particle size distribution. Fourier transform infrared spectroscopy (FT-IR) was used to analyze the functional groups of fibers. A spectrometer

(Nicolet 6700, Thermo Fisher, USA) was used. For the determination of the crystalline cellulose in fibers, X-ray diffraction (XRD) diagram was used. An X-ray diffractometer (D 8, Bruker, USA) in a scan rate of  $0.02^\circ \text{ s}^{-1}$  ( $3\text{--}60^\circ$ ) was used. The amount of crystalline cellulose was calculated by the Eq. (1) [24].

$$\text{CrI}(\%) = \frac{I_{002} - I_{am}}{I_{002}} \times 100\% \quad (1)$$

where  $I_{002}$  is the intensity for the crystalline portion of biomass at  $2\theta = 22.5^\circ$  and  $I_{am}$  is the peak for amorphous cellulose at  $2\theta = 18^\circ$ .

### WPC Preparation

The WPC was prepared by a co-rotating twin-screw extruder (Coperion ZSK, Werner & Pfleiderer, Germany). The compositions of WPCs were as follows: 50% of the sugar crops bagasses, 40% of HDPE, 3% of MA-HDPE, 4% of stearic acid and 3% of polyethylene wax. The well mixed powder was extruded. The zones were heated to  $140\text{--}175^\circ\text{C}$ . An injection moulding machine (HTF 120 $\times$ 2, Haitian, China) at  $140\text{--}165^\circ\text{C}$  was used for the standard specimen injection. The pressure was kept at 60 MPa. The specimen prepared with the dimension of 10 mm width  $\times$  80 mm length  $\times$  4 mm thickness were used for flexural test and the specimens with 50 mm gage length and 4 mm thickness were prepared for tensile and elongation test. All the specimens were prepared in the same processing condition.

### Mechanical Properties

The flexural strength and tensile break strength, the flexural modulus and the tensile modulus, as well as the elongation at break were tested according to the GB/T 24508-2009 by a material testing machine (Instron 1185, USA) [25]. The speed of the flexural and the tensile tests were kept at 10 and 20  $\text{mm min}^{-1}$ , respectively. All of the tests were performed in duplicate.

### Physical Properties

The densities of the WPCs were determined by the volume versus weighting according to our previous study [21]. For the evaluation of the water absorption performances, the specimens were submerged in distilled water at room temperature ( $20 \pm 5^\circ\text{C}$ ). The free water on the surface of specimens was removed, and the mass change towards the raw material mass was defined as the water absorption rate.

### Thermal Properties

Differential scanning calorimeter (DSC) and thermogravimetric analysis (TGA) (TGA/DSC/SF1100, Mettler, Switzerland) were used to analyze the thermal properties of the WPCs. The changes of the specimen crystallinity were calculated by the following equation:

$$X_c (\%) = \frac{100 \times \Delta H_m}{\Delta H_m^0 \times w} \quad (2)$$

where  $\Delta H_m^0$  is the enthalpy of 100% HDPE melting,  $\Delta H_m$  is the enthalpy change of crystalline plastics, and  $w$  refers to the weight of polyethylene.

### Weathering Test

The freeze–thaw weathering and the xenon lamp weathering of the WPCs were performed, which were based on GB/T 16422.2–1999 and GB/T 24508-2009, respectively [25, 26]. For the freeze–thaw weathering, after submerged in water for 24 h at room temperature, the specimens were frozen at  $-30^\circ\text{C}$  for another 24 h. Three cycles were practiced. As for xenon lamp weathering, the specimens were aged in an environment with 290–800 nm of radiance ( $550 \text{ W m}^{-2}$ ). The moisture and temperature of the environment were kept at  $50 \pm 5\%$  and  $65 \pm 5^\circ\text{C}$ , respectively. The modulus of rupture (MOR) and modulus of elasticity (MOE) retention rates of the specimens were determined.

### Statistical Data Analysis

Statistical data analysis was carried out using SPSS 20.0 statistical software. Means and standard deviations of data were calculated. One-way analysis of variance (ANOVA) was performed for the analysis of the results in Table 1, and the significance level of 5% was assumed for each analysis.

## Results and Discussions

### Composition and Characterization of the Fibers

The composition of the three kinds of fibers was shown in Table 1. The SCB had the highest cellulose content in different kinds of fibers ( $43.33 \pm 0.28\%$ ). At the same time, the SCB also had the highest hemicellulose content, which might decrease the mechanical strength of the SCB reinforced specimen due to its high hydrophilicity and the loose structure. Furthermore,  $20.51 \pm 1.6$ ,  $21.32 \pm 2.2$  and  $11.90 \pm 0.23\%$  of lignin were tested in the TMB, SSB and SCB, respectively. Compared with TMB and SSB, the lignin content in SCB was much lower than that in TMB and SSB.

**Table 1** Chemical compositions of the three kinds of fibers

Fiber	Cellulose (Mean $\pm$ SD)	Hemicellulose (Mean $\pm$ SD)	Lignin (Mean $\pm$ SD)	Soluble constituent (Mean $\pm$ SD)	Ash (Mean $\pm$ SD)
TMB	25.6 $\pm$ 2.6 <sup>b</sup>	34.6 $\pm$ 3.1 <sup>c</sup>	20.5 $\pm$ 2.1 <sup>b</sup>	17.5 $\pm$ 2.1 <sup>a</sup>	1.9 $\pm$ 0.3 <sup>b</sup>
SSB	30.0 $\pm$ 2.6 <sup>c</sup>	17.3 $\pm$ 2.1 <sup>b</sup>	21.4 $\pm$ 1.8 <sup>c</sup>	29.6 $\pm$ 1.2 <sup>b</sup>	1.7 $\pm$ 0.3 <sup>a</sup>
SCB	14.8 $\pm$ 1.8 <sup>a</sup>	15.5 $\pm$ 1.7 <sup>a</sup>	16.3 $\pm$ 1.7 <sup>a</sup>	48.6 $\pm$ 3.2 <sup>c</sup>	4.8 $\pm$ 0.4 <sup>c</sup>

SD standard deviation

<sup>a,b,c</sup>Values with the same superscript letters were not significantly different

$P > 0.05$

It has been reported that lignin in the reinforcement phase could increase the mechanical and thermal properties of the polymer matrices [27]. As can be seen in Table 1, the soluble component contents in TMB and SSB were higher than that in SCB. Therefore, the SCB reinforced specimen might provide better mechanical thermal properties.

The fiber size has significant effect on the dispersion of fibers in polymer matrix, and the properties of WPC were further affected [28]. The results of fibers' particle size distributions were shown in Fig. 1c and the average particle size of each fiber was listed in Table 2. The SEM was employed to observe the morphology of fibers. As can be seen from Table 2, the SCB had the longest diameter among three fibers (402.125  $\mu\text{m}$ ), the diameter of TMB was the shortest (140.378  $\mu\text{m}$ ), and SSB fiber was longer than TMB (256.32  $\mu\text{m}$ ). It has been reported that the mechanical properties of the composites increased first and then decreased with the increase of the particle size [29–31]. The morphology of fibers was shown in Fig. S1. The SSB fiber had bold outline and the largest aspect ratio compared with other fibers. Fibers with high aspect ratio in composites enhanced tensile strength and tensile modulus of the composites [32].

FTIR was used to examine the functional groups present in the fibers. Figure 1a shows the FTIR spectra of TMB, SSB and SCB. All the fibers have strong hydrogen bonded O–H stretching absorption at around 3400  $\text{cm}^{-1}$ . The peak located at 1240 and 1738  $\text{cm}^{-1}$  which belong to the C–O and C=O stretching vibration were characteristics for hemicelluloses, respectively [33]. The peaks at 1514 and 1605  $\text{cm}^{-1}$  belonged to the C=C aromatic ring skeleton stretching vibration, indicating that the presence of lignin in the fibers structure. The peak located at 1053  $\text{cm}^{-1}$  belonged to the C–O–C stretching vibration of cellulose. As it indicated in Fig. 1a, there is no significant discrepancy in the functional groups of the three fibers.

The changes in cellulose structure after physicochemical and biological pretreatments could be interpreted according to the crystallinity index (CrI) [21, 34]. XRD is a well-established method for measuring the crystallinity of the entire fiber including the hemicellulose, lignin and amorphous cellulose [35]. Cellulose is composed of crystalline

and amorphous region inside the lignocellulosic fibers [36]. Besides, hemicellulose and lignin provides amorphous structures [34].

The XRD patterns of TMB, SCB and SSB are shown in Fig. 1b. The crystallinity index (CrI) of lignocellulosic fibers was calculated according to the XRD patterns (Table 3). Although the cellulose content of SCB was the highest among the fibers, the CrI of SCB was the lowest. This might be attributed to the highest hemicellulose and lignin content in SCB (see Table 1). Besides, the amorphous region in cellulose of SCB was relatively high. It has been proved that the crystallinity is a crucial factor to WPC since it affects the thermal stability and the mechanical properties of the fibers [37].

## Mechanical Properties

Figure 2 demonstrates the properties of the specimens reinforced by different types of fibers. As can be seen, the mechanical properties of the specimen reinforced by SCB were poorer compared to the specimens prepared reinforced by TMB and SSB. This phenomenon could be attributed to the lower content of lignin and higher content of hemicellulose in SCB. Hemicellulose is the most unstable, amorphous and hydrophilic component in fibers, which has negative effects on the mechanical strength of fibers and the composites. In addition, lignin has positive effect on the interfacial adhesion between fibers and polymer matrix and thermal stabilities of composites [33]. The lower content of the cellulose is in fiber, the looser structure of fiber and the low-intensity specimens obtained [21]. However, in comparison with the specimen that reinforced by TMB, the flexural strength of specimen reinforced by SSB was little lower (46.10  $\pm$  3.1 MPa for TMB group and 42.46  $\pm$  2.6 MPa for SSB group), though the cellulose content in SSB is higher than that in TMB (34.65  $\pm$  4.2% for TMB and 38.47  $\pm$  3.2% for SSB). It was attributed to the little higher lignin in SSB (21.32  $\pm$  2.2%). The component with large modulus of elasticity was beneficial to the flexural strength while lignin is a particle with high modulus [38].

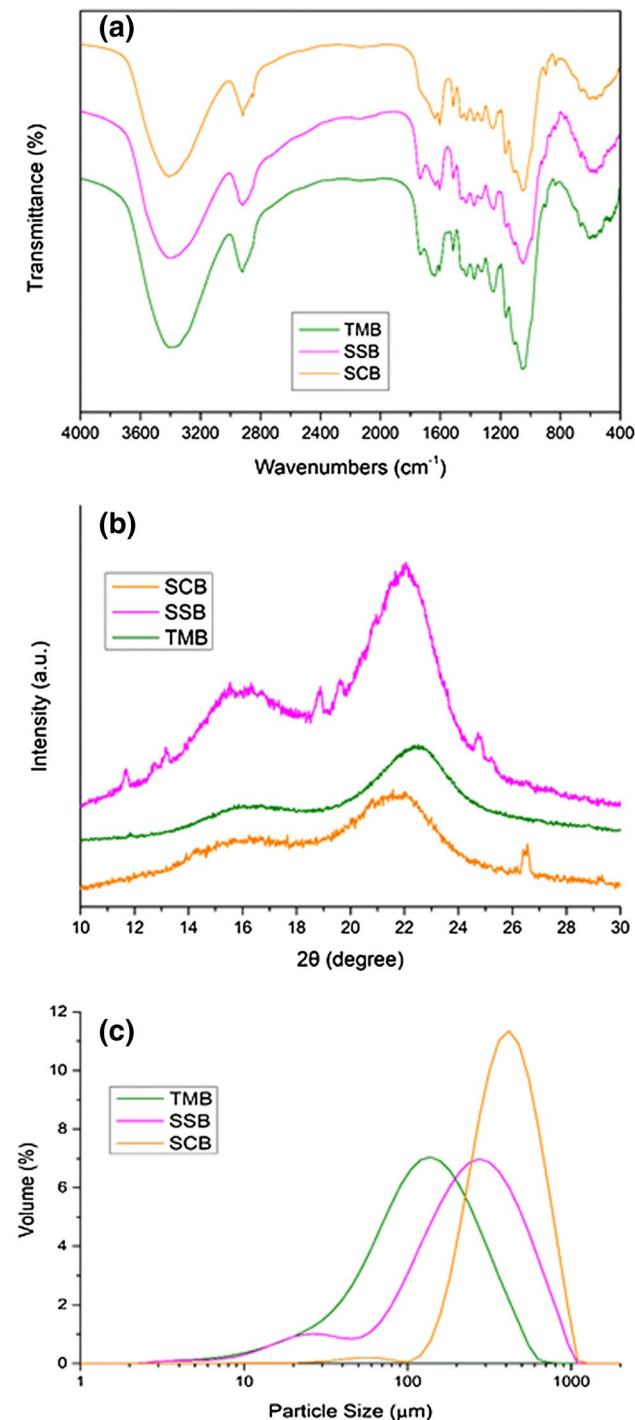


**Fig. 1** Characterization of the three kinds of fibers. **a** FT-IR; **b** XRD; **c** Particle size distribution

In contrast, the highest tensile and flexural modulus was obtained in the group that reinforced by SSB ( $3227.98 \pm 236.7$  MPa of tensile modulus and  $4151.66 \pm 219.3$  MPa of flexural modulus). This is due to the highest cellulose content and lignin content in SSB ( $38.47 \pm 3.2\%$  of cellulose and  $21.32 \pm 2.2\%$  of lignin). It

**Table 2** Particle size distribution

Particle	Average particle size ( $\mu\text{m}$ )
TMB	140.378
SSB	256.562
SCB	402.125

**Table 3** Crystallinity characteristics of different fibers

Fibers	TMB	SSB	SCB
$I_{002}$	10,496	42,716.7	22,216.7
$I_{am}$	5718	24,000	14,400
CrI	45.5%	43.8%	35.2%

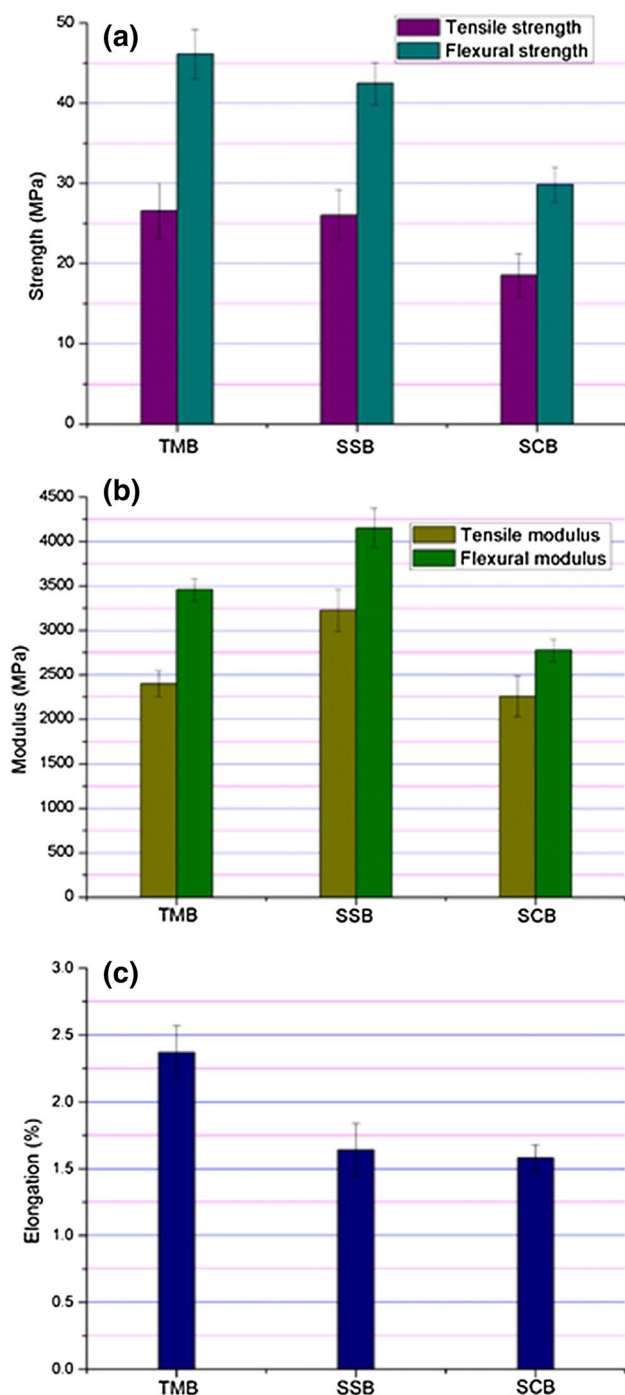
evidenced that cellulose has a positive effect on the tensile modulus and flexural modulus [39], while lignin is a particle with high modulus [38].

Figure 2c shows the elongation at break of the specimens reinforced by the fibers. As can be seen, the elongation at break of the specimens reinforced by TMB was the highest and was much higher than that of the other specimens. This can be explained by the high content of lignin and soluble fraction in TMB (see Table 1). Previous works demonstrated that the higher content of lignin in lignocellulosic fibers results in the increased adhesion effects towards polymers [40]. Additionally, some lipophilic soluble fraction also affected the dispersion of the particles in the process of WPC preparation [41]. Hence, the soluble fraction is likely to contribute to the high elongation at break.

## Physical Properties

The moisture absorbability of WPCs was mainly caused by the hydrophilic character of the reinforcement phase [42]. The water adsorption rate of the three specimens all met the national standard (below 3%) (Fig. 3a) [21]. There are abundant free hydroxyl groups in fibers. The free hydroxyl groups could interact with water molecules by hydrogen bonding. The key factor of water absorption of composites is the availability of free hydroxyl groups on the surface of fibers. As it demonstrated in literature, hemicellulose is the most hydrophilic component of wood fiber [43]. As it shown in Fig. 3a, the water absorption of SCB reinforced specimen was higher than other two specimens. This is attributed to the highest content of hemicellulose in TMB, as it showed in Table 1.

The WPC density is mainly associated with the density of fibers. In the case of commercialization, light weight material is more attractive because of the advantages of easy handling and low transportation costs [44]. Figure 3b shows the



**Fig. 2** Mechanical properties of the different kinds of fibers reinforced composites. **a** flexural strength and tensile strength; **b** flexural modulus and tensile modulus; **c** elongations

densities of the specimens reinforced by different types of fibers. As can be seen, there were no obvious differences of WPCs density among the three kinds of specimens. All the specimens met the national standard for the density of WPCs ( $0.85 \text{ g cm}^{-3}$ ). Therefore, the chemical composition between the fibers had no significant effect on density of WPC.

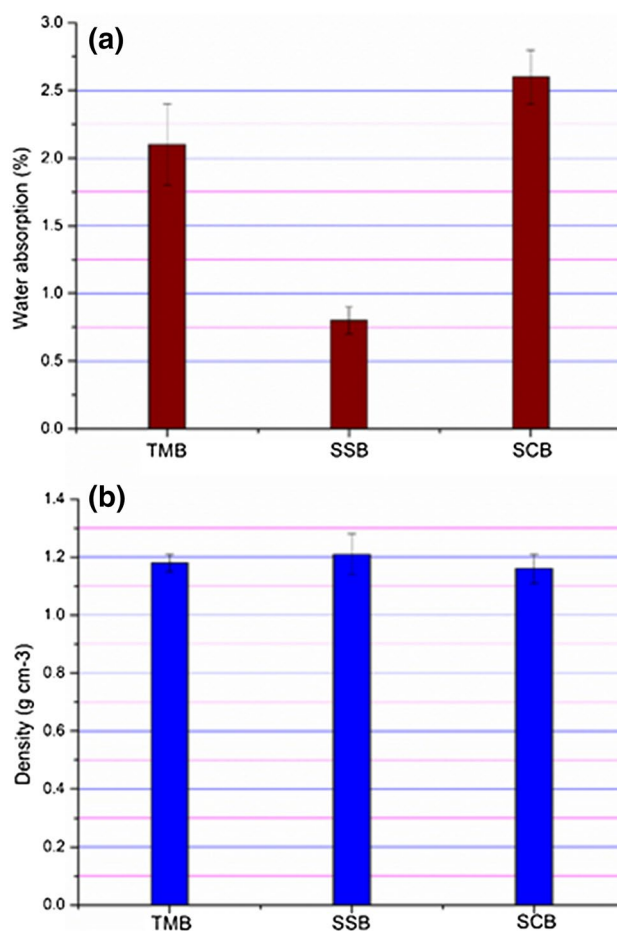


**Fig. 3** Physical properties of the different kinds of fibers reinforced composites. **a** Water absorption; **b** density

### Thermal Properties

Thermal properties of WPCs were evaluated to interpret the thermal stability and decomposition mechanism of the composites. Figure 4 shows the TGA and DTG curves of the specimens. There were generally three steps in the decomposition procedure of the composites. Generally, the weight loss at temperature below  $100 \text{ }^\circ\text{C}$  was attributed to the evaporation or dehydration of loosely bound water and low molecular weight compound [45]. For the chemical components of the fibers, according to Tomczak et al. [46] research, cellulose was degraded between  $240$  and  $350 \text{ }^\circ\text{C}$ , hemicellulose was degraded between  $200$  and  $260 \text{ }^\circ\text{C}$ , and lignin was degraded between  $280$  and  $500 \text{ }^\circ\text{C}$ .

Figure 4b shows the mass loss rate of the composites. In comparison with the specimens based on TMB and SSB, the maximum mass loss rate in first peak of the mass loss curve of the SCB specimen was slightly shifted to higher temperature. It might be associated with the relatively high levels of cellulose in SCB. Moreover, it very interesting that the residual of the three specimens at  $600 \text{ }^\circ\text{C}$  were much

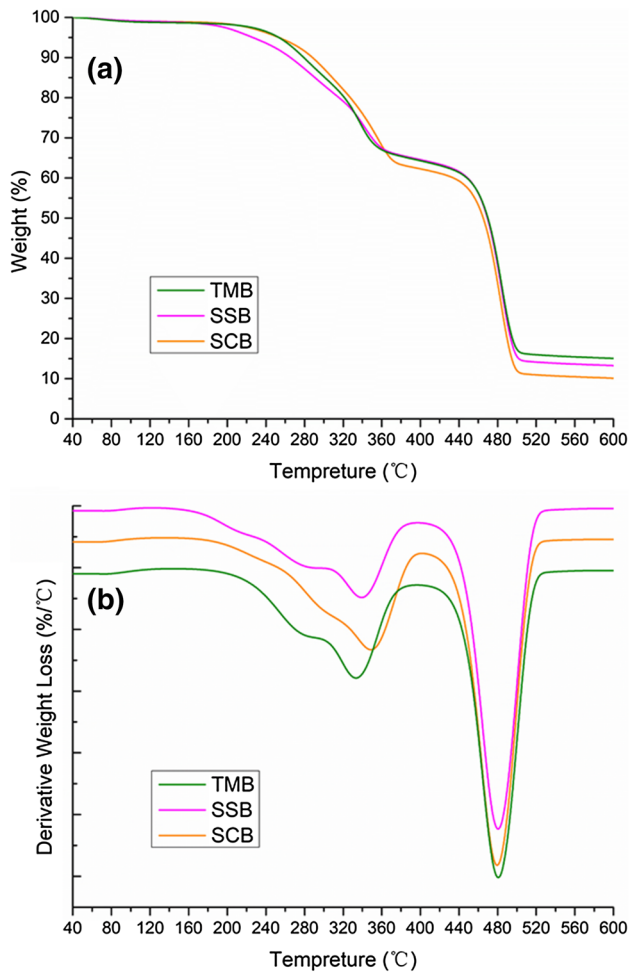


Fig. 4 TGA thermograms of the different kinds of fibers reinforced composites. a TG curves; b DTG curves

higher than the corresponding ash content in the crude fibers (see Fig. 1a). It is because ashes in the fibers were tested in oxygen atmosphere. On this condition, most of the oxides were oxidatively decomposed. Instead, the TGA is heated in nitrogen atmosphere and the ash includes carbide that could not be oxide after treatment.

Table 4 summarizes the TGA results of the specimens reinforced by different types of fibers. As it indicated, SCB reinforced specimen has 10% weight loss temperature and 50% weight loss temperature. It was due to the highest cellulose content in SCB compared with other fibers. This indicated that the high content of cellulose in fibers led to the improvement of the thermal stability of WPCs, which was also indicated in previous study [47].

The melting and crystallization behaviors of the WPCs reinforced by TMB, SSB and SCB and pure HDPE were further evaluated. The DSC curve the composites were shown in Fig. 5. And the results of DSC were also summarized in Table 5. According to the results, the  $X_c$  and  $T_c$  of the

Table 4 TGA results of the specimens reinforced by different types of fibers

Samples	L-10% (°C) <sup>a</sup>	L-50% (°C) <sup>a</sup>	Weight loss (wt%)	Residual at 600 °C (wt%)
TMB	279	465	84.9	15.1
SSB	259	469	86.7	13.3
SCB	288	470	89.9	10.1

<sup>a</sup>L-10%, L-50% represents the 10% weight loss temperature and the 50% weight loss temperature, respectively

specimens were increased after adding the reinforced phases. The increase of  $X_c$  indicated that the reinforced phases acted as the nucleating agent in the crystallization. Furthermore, the increase of  $T_c$  demonstrated that the addition of fibers accelerated the crystallization process [48]. In comparison with the pure matrix, the melting temperature ( $T_m$ ) of the

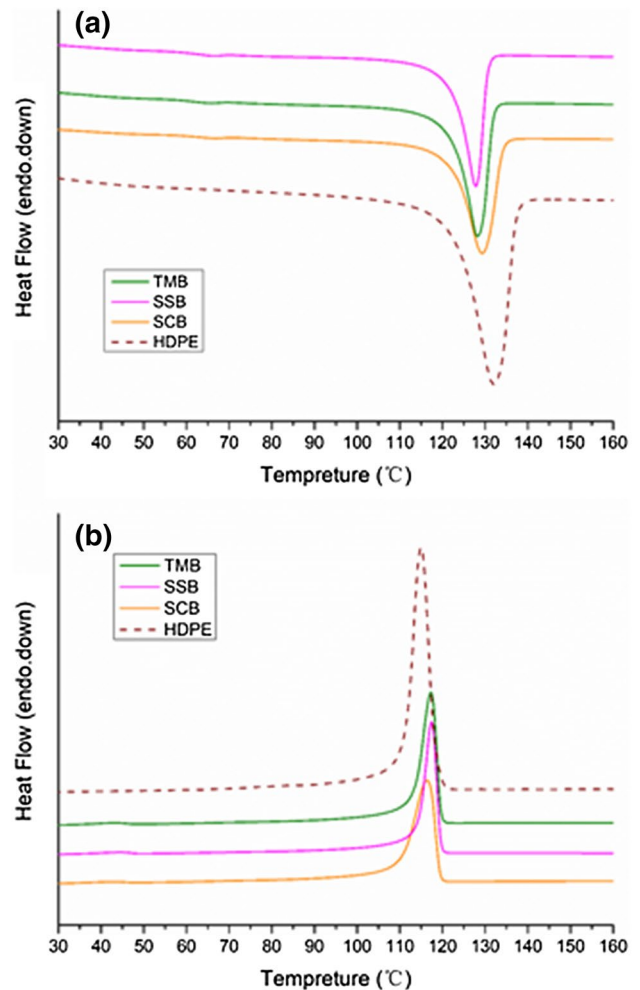


Fig. 5 The melting point temperatures and the crystallization temperatures of the different kinds of fibers reinforced composites. a The melting point temperatures; b the crystallization temperatures

**Table 5** The results of differential scanning calorimetry (DSC) analysis

Fibers	TMB	SSB	SCB	HDPE
$T_m$ (°C)	129.2	129.03	130.44	130.59
$T_c$ (°C)	117.93	117.93	117.17	116.24
$\Delta H_c$ (J g <sup>-1</sup> )	73.66	63.07	73.51	146.84
$\Delta H_m$ (J g <sup>-1</sup> )	75.76	67.26	79.34	148.95
$X_c$ (%)	65.6	58.2	68.7	50.8

WPCs was decreased. It suggested that the perfection of matrix crystallites was decreased due to the heterogeneous nucleation that promoted by the presence of the fibers [49]. Table 5 also showed that the enthalpy of HDPE was especially high (146.84 J g<sup>-1</sup>). In the TMB, SSB and SCB reinforced specimens, the melting enthalpies ( $\Delta H_m$ ) were significantly decreased to 67.26–79.34 J g<sup>-1</sup>. It is because the fibers act as a diluent fraction in the HDPE matrix [50, 51].

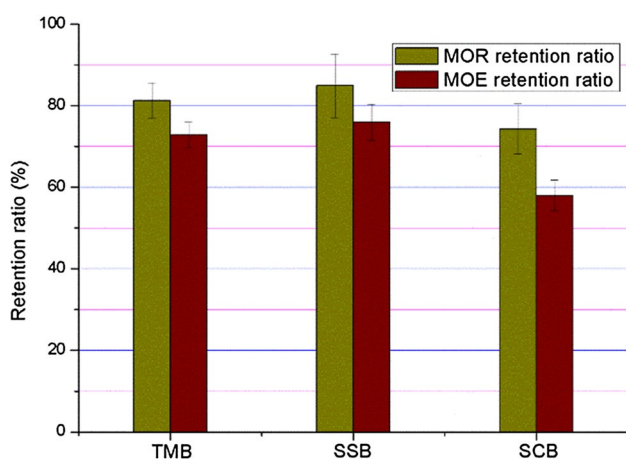
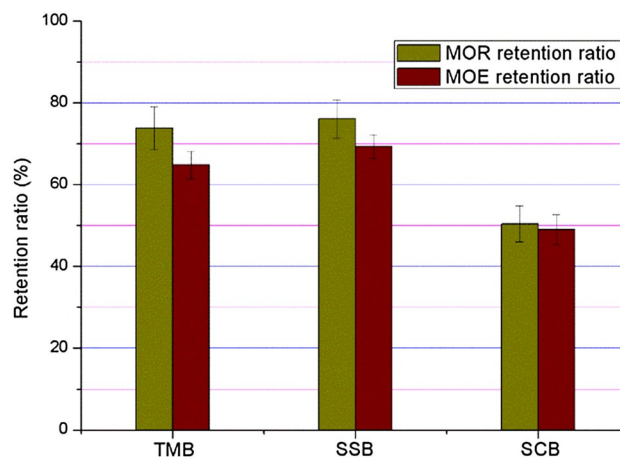
### Weathering Test

Flexural strength (MOR) and flexural stiffness (MOE) showed a crucial role in the performance of WPCs in the cases of realistic using [52]. The MOR and MOE retention ratio of the specimens that exposed to three freeze–thaw cycles were shown in Fig. 6. It showed the MOR and MOE in all specimens were significantly reduced. It is attributed to the degradation of interfacial adhesion due to the moisture absorption [53]. In addition, the MOR and MOE retention ratio in the SCB reinforced specimen was lower than that in TMB and SSB reinforced specimens. This phenomenon could be assign to the high hemicellulose content and low lignin content in SSB. During the process of the freeze–thaw exposure, the specimens cycled through water absorption and freezing, which would severely damage the structure of

composites. However, lignin has weak hydrophilicity and provides mechanical strength for the cell walls [21]. Therefore, the reinforcement phase with higher lignin content was not easy to degrade, leading to the enhancement of the specimens' stability.

SEM was carried out to qualitatively determine the effects of freeze–thaw cycles on the surface properties of specimens. Figs. S2, S3 showed the surface of specimens before and after freeze–thaw cycles, respectively. It indicated that the repeated freeze–thaw had a great impact on the performance of the composites. For the untreated samples, the SEM image (Fig. S2) showed the defects of the specimens' surface were mainly composed by small holes [54]. After weathering, big cracks were arisen on the surface of the freeze–thawed specimens, which indicated a loss of bonding between the fibers and the matrix was obtained after weathering.

The MOR and MOE retention ratio of the specimens after the xenon lamp weathering are shown in Fig. 7. After 2000 h of weathering, MOR and MOE in all groups were decreased significantly. It was ascribed to a chain scission mechanism by photo degradation of the HDPE [55]. More significantly, the MOR and MOE retention ratio in the SCB reinforced specimens were much lower compared with the results in the TMB and SSB based groups. It was attributed to the low lignin content in SCB. The lignin contained numerous chromophores that showed possibility to absorb UV radiation effectively [56]. However, though the lignin content in SSB and TMB were at the same level, the MOR and MOE retention ratio in TMB based specimen was still lower than that of the SSB based specimen. This might be assign to the higher content of hemicellulose in TMB. The xenon lamp weathering lead to the oxidization and the degradation of hemicelluloses after artificial photo-weathering which caused the low MOR and MOE retention ratios in the TMB group [57, 58].

**Fig. 6** MOR and MOE retention ratios after multigelation**Fig. 7** MOR and MOE retention ratios after xenon lamp weathering



## Conclusions

In this paper, three types of biomass residues were studied and evaluated for the preparation of WPCs. Results indicated that the TMB reinforced composites showed better mechanical properties than other biomass residues reinforced WPCs. Besides, the SSB reinforced composites had better performance in the aspect of long-term stability due to the high content of lignin in SSB. These results demonstrated that the WPCs production could be connected with the bio-fuels plant using the sugar contain juices as substrate.

**Acknowledgements** This work was supported in part by the National Nature Science Foundation of China (Grant No. 21706008), China Postdoctoral Science Foundation (Grant Nos. 2017M610037; 2018T110036) and the Fundamental Research Funds for the Central Universities (Grant No. ZY 1832).

## References

1. Youssef, A.M., El-Gendy, A., Kamel, S.: Evaluation of corn husk fibers reinforced recycled low density polyethylene composites. *Mater. Chem. Phys.* **152**, 26–33 (2015)
2. Zahedi, M., Tabarsa, T., Ashori, A., Madhoushi, M., Shakeri, A.: A comparative study on some properties of wood plastic composites using *Canola* stalk, *Paulownia*, and nanoclay. *J. Appl. Polym. Sci.* **3**, 1491–1498 (2013)
3. Ayrlimis, N., Kaymakci, A.: Fast growing biomass as reinforcing filler in thermoplastic composites: *Paulownia elongate* wood. *Ind. Crop. Prod.* **43**, 457–464 (2013)
4. Georgopoulos, S.T., Tarantili, P.A., Avgerinos, E., Andreopoulos, A.G., Koukios, E.G.: Thermoplastic polymers reinforced with fibrous agricultural residues. *Polym. Degrad. Stab.* **90**, 303–312 (2005)
5. Correll, D., Suzuki, Y., Martens, B.J.: Logistical supply chain design for bioeconomy applications. *Biomass Bioenergy* **66**, 60–69 (2014)
6. Láinez, J.M., Puigjaner, L.: Prospective and perspective review in integrated supply chain modeling for the chemical process industry. *Curr. Opin. Chem. Eng.* **1**, 430–445 (2012)
7. Wei, L., Liang, S., McDonald, A.G.: Thermophysical properties and biodegradation behavior of green composites made from polyhydroxybutyrate and potato peel waste fermentation residue. *Ind. Crop. Prod.* **69**, 91–103 (2015)
8. Madbouly, S.A., Schrader, J.A., Srinivasan, G., Liu, K., McCabe, K.G., Grewell, D., Graves, W.R., Kessler, M.R.: Biodegradation behavior of bacterial-based polyhydroxyalkanoate (PHA) and DDGS composites. *Green Chem.* **16**, 1911–1920 (2014)
9. Muniyasamy, S., Reddy, M.M., Misra, M., Mohanty, A.: Biodegradable green composites from bioethanol co-product and poly (butylenesadipate-co-terephthalate). *Ind. Crop. Prod.* **43**, 812–819 (2013)
10. Torres, S., Navia, R., Murdy, R.C., Cooke, P., Misra, M., Mohanty, A.K.: Green composites from residual microalgae biomass and poly (butylenesadipate-co-terephthalate): processing and plasticization. *ACS Sustain. Chem. Eng.* **3**, 614–624 (2015)
11. Yu, J., Zhang, T., Zhong, J., Zhang, X., Tan, T.: Biorefinery of sweet sorghum stem. *Biotechnol. Adv.* **30**, 811–816 (2012)
12. Sarkar, N., Ghosh, S.K., Bannerjee, S., Aikat, K.: Bioethanol production from agricultural wastes: an overview. *Renew. Energy* **37**, 19–27 (2012)
13. Behera, S., Arora, R., Nandhagopal, N., Kumar, S.: Importance of chemical pretreatment for bioconversion of lignocellulosic biomass. *Renew. Sustain. Energy Rev.* **36**, 91–106 (2014)
14. Zhai, R., Hu, J., Saddler, J.N.: What are the major components in steam pretreated lignocellulosic biomass that inhibit the efficacy of cellulase enzyme mixtures? *ACS Sustain. Chem. Eng.* **4**, 3429–3436 (2016)
15. Cai, D., Chang, Z., Wang, C., Ren, W., Wang, Z., Qin, P., Tan, T.: Impact of sweet sorghum cuticular waxes (SSCW) on acetone-butanol-ethanol fermentation using *Clostridium acetobutylicum* ABE 1201. *Bioresour. Technol.* **149**, 470–473 (2013)
16. Jiang, W., Zhao, J., Wang, Z., Yang, S.T.: Stable high-titer n-butanol production from sucrose and sugarcane juice by *Clostridium acetobutylicum* JB 200 in repeated batch fermentations. *Bioresour. Technol.* **163**, 172–179 (2014)
17. Chang, Z., Cai, D., Wang, Y., Chen, C., Fu, C., Wang, G., Qin, P., Wang, Z., Tan, T.: Effective multiple stages continuous acetone-butanol-ethanol fermentation by immobilized bioreactors: making full use of fresh corn stalk. *Bioresour. Technol.* **205**, 82–89 (2016)
18. Nguyen, T.L.T., Hermansen, J.E.: System expansion for handling co-products in LCA of sugar cane bio-energy systems: GHG consequences of using molasses for ethanol production. *Appl. Energy* **89**, 254–261 (2012)
19. Pellegrini, L.F., de Oliveira Junior, S.: Combined production of sugar, ethanol and electricity: thermo economic and environmental analysis and optimization. *Energy* **36**, 3704–3715 (2011)
20. Zhong, J., Zhang, L., Yu, J., Tan, T., Zhang, X.: Studies of different kinds of fiber pretreating on the properties of PLA/sweet sorghum fiber composites. *J. Appl. Polym. Sci.* **117**, 1385–1393 (2010)
21. Luo, Z., Li, P., Cai, D., Chen, Q., Qin, P., Tan, T., Cao, H.: Comparison of performances of corn fiber plastic composites made from different parts of corn stalk. *Ind. Crop. Prod.* **95**, 521–527 (2017)
22. Klímeček, P., Meinschmidt, P., Wimmer, R., Plinke, B., Schirp, A.: Using sunflower (*Helianthus annuus* L.), topinambour (*Helianthus tuberosus* L.) and cup-plant (*Silphium perfoliatum* L.) stalks as alternative raw materials for particleboards. *Ind. Crop. Prod.* **92**, 157–164 (2016)
23. Sluiter, A., Hames, B., Ruiz, R., Scarlata, C., Sluiter, J., Templeton, D., Crocker, D.: Determination of structural carbohydrates and lignin in biomass. Laboratory Analytical Procedure, NREL, Report No. TP-510-42618: (2008)
24. Segal, L., Creely, J.J., Martin, A.E., Conrad, C.M.: An empirical method for estimating the degree of crystallinity of native cellulose using the X-ray diffractometer. *Text. Res. J.* **29**, 786–794 (1959)
25. Wang, H.Y., Li, D.G., Wang, Y.M., Lin, D.L.: Cross-sectional stiffness analysis and support span calculation of WPC decking. *Appl. Mech. Mater.* **170**, 3175–3180 (2012)
26. Meng, J., Wang, Y.: Effect of xenon arc lamp irradiation on properties of polymethyl methacrylate for aviation. *Open J. Org. Polym. Mater.* **5**, 23 (2015)
27. Shankar, S., Reddy, J.P., Rhim, J.W.: Effect of lignin on water vapor barrier, mechanical, and structural properties of agar/lignin composite films. *Int. J. Biol. Macromol.* **81**, 267–273 (2015)
28. Zykova, A.K., Pantyukhov, P.V., Kolesnikova, N.N., Popov, A.A., Olkhov, A.A.: Influence of particle size on water absorption capacity and mechanical properties of polyethylene-wood flour composites. *AIP Conf.* **1683**, 41–688 (2015)
29. Verhey, S.A., Laks, P.E.: Wood particle size affects the decay resistance of woodfiber/thermoplastic composites. *For. Prod. J.* **52**, 78–81 (2002)
30. Chen, H.C., Chen, T.Y., Hsu, C.H.: Effects of wood particle size and mixing ratios of hdpe on the properties of the composites. *Holz. Roh. Werkst.* **64**, 172–177 (2006)

31. Maiti, S.N., Singh, K.: Influence of wood flour on the mechanical properties of polyethylene. *J. Appl. Polym. Sci.* **32**, 4285–4289 (1986)
32. Dayo, A.Q., Wang, A.R., Kiran, S., Wang, J., Qureshi, K., Xu, Y.L., Zegaoui, A., Derradji, M., Babar, A.A., Liu, W.B.: Impacts of hemp fiber diameter on mechanical and water uptake properties of polybenzoxazine composites. *Ind. Crop. Prod.* **111**, 277–284 (2017)
33. Liu, R., Peng, Y., Cao, J., Chen, Y.: Comparison on properties of lignocellulosic flour/polymer composites by using wood, cellulose, and lignin flours as fillers. *Compos. Sci. Technol.* **103**, 1–7 (2014)
34. Bernardinelli, O.D., Lima, M.A., Rezende, C.A., Polikarpov, I., de Azevedo, E.R.: Quantitative <sup>13</sup>C multi CP solid-state NMR as a tool for evaluation of cellulose crystallinity index measured directly inside sugarcane biomass. *Biotechnol. Biofuels* **8**, 1–11 (2015)
35. Kim, S., Holtzapple, M.T.: Effect of structural features on enzyme digestibility of corn stover. *Bioresour. Technol.* **97**, 583–591 (2006)
36. Liitiä, T., Maunu, S.L., Hortling, B., Tamminen, T., Pekkala, O., Varhimo, A.: Cellulose crystallinity and ordering of hemicelluloses in pine and birch pulps as revealed by solid-state NMR spectroscopic methods. *Cellulose* **10**, 307–316 (2003)
37. Hoi, L.W.S., Martincigh, B.S.: Sugar cane plant fibres: separation and characterisation. *Ind. Crop. Prod.* **47**, 1–12 (2013)
38. Toriz, G., Denes, F., Young, R.A.: Lignin-polypropylene composites. Part 1: Composites from unmodified lignin and polypropylene. *Polym. Composite* **23**, 806–813 (2010)
39. John, M.J., Anandjiwala, R.D.: Recent developments in chemical modification and characterization of natural fiber-reinforced composites. *Polym. Composite* **29**, 187–207 (2010)
40. Morandim-Giannetti, A.A., Agnelli, J.A.M., Lanças, B.Z., Magnabosco, R., Casarin, S.A., Bettini, S.H.P.: Lignin as additive in polypropylene/coir composites: thermal, mechanical and morphological properties. *Carbohydr. Polym.* **87**, 2563–2568 (2012)
41. Sheshmani, S., Ashori, A., Farhani, F.: Effect of extractives on the performance properties of wood flour-polypropylene composites. *J. Appl. Polym. Sci.* **123**, 1563–1567 (2012)
42. Hosseinaei, O., Wang, S., Taylor, A.M., Kim, J.W.: Effect of hemicellulose extraction on water absorption and mold susceptibility of wood-plastic composites. *Int. Biodeter. Biodegr.* **71**, 29–35 (2012)
43. Godvarti, S.: Thermoplastic wood fiber composites. In: Mohanty, A.K., Misra, M., Drzal, L.T. (eds.) *Natural fibers, biopolymers and biocomposites*, pp. 347–389. Taylor & Francis Group, Boca Raton (2005)
44. Jumaidin, R., Sapuan, S.M., Jawaid, M., Ishak, M.R., Sahari, J.: Thermal, mechanical, and physical properties of seaweed/sugar palm fibre reinforced thermoplastic sugar palm starch/agar hybrid composites. *Int. J. Biol. Macromol.* **97**, 606 (2017)
45. Sanyang, M.L., Sapuan, S.M., Jawaid, M., Ishak, M.R., Sahari, J.: Effect of plasticizer type and concentration on tensile, thermal and barrier properties of biodegradable films based on sugar palm (*Arenga pinnata*) starch. *Polymers* **7**, 1106–1124 (2015)
46. Tomczak, F., Sydenstricker, T.H.D., Satyanarayana, K.G.: Studies on lignocellulosic fibers of Brazil. Part II: morphology and properties of Brazilian coconut fibers. *Compos. Part A-Appl. Sci. Manufact.* **38**, 1710–1721 (2007)
47. Fabyi, J.S., McDonald, A.G.: Effect of wood species on property and weathering performance of wood plastic composites. *Compos. Part A-Appl. Sci. Manufact.* **41**, 1434–1440 (2010)
48. Joseph, P.V., Joseph, K., Thomas, S., Pillai, C.K.S., Prasad, V.S., Groeninckx, G., Sarkissova, M.: The thermal and crystallisation studies of short sisal fibre reinforced polypropylene composites. *Compos. Part A-Appl. Sci. Manuf.* **34**, 253–266 (2003)
49. Sarasini, F., Tirillò, J., Serji, C., Seghini, M.C., Cozzarini, L., Graupner, N.: Effect of basalt fibre hybridisation and sizing removal on mechanical and thermal properties of hemp fibre reinforced HDPE composites. *Compos. Struct.* **188**, 394–406 (2018)
50. Amash, A., Zugenmaier, P.: Morphology and properties of isotropic and oriented samples of cellulose fibre-polypropylene composites. *Polymer* **41**, 1589–1596 (2000)
51. Arbelaiz, A., Fernández, B., Ramos, J.A., Mondragon, I.: Thermal and crystallization studies of short flax fibre reinforced polypropylene matrix composites: effect of treatments. *Thermochim. Acta* **440**, 111–121 (2006)
52. Lopez, J.L., Sain, M., Cooper, P.: Performance of natural-fiber-plastic composites under stress for outdoor applications: effect of moisture, temperature, and ultraviolet light exposure. *J. Appl. Polym. Sci.* **99**, 2570–2577 (2010)
53. Panthapulakkal, S., Law, S., Sain, M.: Effect of water absorption, freezing and thawing, and photo-aging on flexural properties of extruded HDPE/rice husk composites. *J. Appl. Polym. Sci.* **100**, 3619–3625 (2006)
54. Pilarski, J.M., Matuana, L.M.: Durability of wood flour-plastic composites exposed to accelerated freeze-thaw cycling. Part I. Rigid PVC matrix. *J. Vinyl. Addit. Tech.* **11**, 1–8 (2005)
55. Soccalingame, L., Perrin, D., Bénézet, J.C., Bergeret, A.: Reprocessing of UV-weathered wood flour reinforced polypropylene composites: study of a natural outdoor exposure. *Polym. Degrad. Stabil.* **133**, 389–398 (2016)
56. Chaochanchaikul, K., Jayaraman, K., Rosarpitak, V., Sombatsompop, N.: Influence of lignin content on photodegradation in wood/HDPE composites under UV weathering. *Bioresources* **7**, 38–55 (2012)
57. Liu, R., Pang, X., Yang, Z.: Measurement of three wood materials against weathering during long natural sunlight exposure. *Measurement* **102**, 179–185 (2017)
58. Chen, Y., Stark, N.M., Tshabalala, M.A., Gao, J., Fan, Y.: Weathering characteristics of wood plastic composites reinforced with extracted or delignified wood flour. *Materials* **9**, 610 (2016)